Wireless Tomography, Part II: A System Engineering Approach

R. C. Qiu*, Z. Hu*, M. C. Wicks†, S. J. Hou*, L. Li*, and J. L. Gary *
*Cognitive Radio Insitute, Department of Electrical and Computer Engineering,
Center for Manufacturing Research, Tennessee Technological University,
Cookeville, Tennessee, Email: rqiu@tntech.edu
†Air Force Research Laboratory, Sensors Directorate, Rome, New York
Email: Michael.Wicks@rl.af.mil

***Abstract*—This is the second paper in a series on a new initiative of wireless tomography. The goal is to combine two areas: wireless communication and radio tomography. This paper studies wireless tomography from a system engineering's point of view. Machine learning and waveform diversity will be applied to wireless tomography. The potential system architecture for wireless tomography will also be given.**

***Index Terms*—wireless tomography, machine learning, waveform diversity**

I. Introduction

This is Part II of the paper series [1], [2]. Wireless tomography is a novel approach to remote sensing. This idea—combining the wireless communications and remote sensing—is based on many years research insight. The methodology, literature review and related work, and open problems are presented in Part I [1].

When only communications components are used for system development, the phase of the signal is either inaccurate or very expensive to obtain. We suggest self-coherent wireless tomography, which has two steps. First, the phase retrieval is achieved using amplitude only data that are obtained through wireless sensors. Second, standard radio tomographic imaging algorithms are used for data analysis.

Our goal is to design a self-coherent wireless tomography system. To achieve this goal, there are two important problems in system engineering. The first problem is the measurement error introduced by Commercial, Off-The-Shelf (COTS) communication components. The second is to design a waveform to achieve the system performance.

A. Improving Phase Reconstruction Using Machine Learning

To fix ideas, let us consider the two algorithms that are given in Section III of Part I [1]. Only a finite number of degrees of freedom (finite dimensions), N_{DOF}, needs to be retrieved in the phase reconstruction problem. For example, $N_{DOF} = 241$ is used in the case studied in [1]. When COTS communication components are used, measurement errors in amplitude (attenuation) are difficult to control. As a result, this is a basic problem using our new architecture to retrieve the phase via reconstruction so that coherent tomographic processing can be enabled (justifying the acronym self-coherent tomography).

Fortunately, the size of the sample space is large so that machine learning can be applied to reduce the dimensionality of the problem. The random errors introduced by the COTS components tend to be large, compared with the finite dimensions. Thus, we introduce a new step called machine learning, before the phase reconstruction step and the coherent tomographic processing step are applied. This new three-step approach is natural.

Indeed, affordable computing and low-cost COTS communication sensors are behind this three-step approach. We can trade COTS sensors for the expensive Ad Hoc sensor networks.

B. Waveform Diversity in Wireless Tomography

Waveform diversity is a key research issue in wireless communications,radar, and sensing or imaging systems. Waveforms should be designed or optimized according to different requirements or objectives for system performance and should be adapted to the operating environment in order to achieve performance gain [3]. For example, waveforms should be designed to carry more information to the receiver in terms of mutual information. If an energy detector is employed at the receiver, waveforms should be optimized such that the energy of the signal in the integration window reaches the maximum [4] [5] [6] [7]. For navigation and geolocation, an ultra short waveform should be used to increase resolution. For multi-target identification, waveforms may be designed such that the radar returns can provide more target information. In clutter dominant environments, maximizing the target energy and minimizing the clutter energy should be a priority.

Besides waveform diversity at the transmitter, any type of waveform level signal processings at the receiver should also be included within the waveform diversity framework. For example, adaptive filters or notch filters can be designed to cancel the interference. In acoustic communications, passive time reversal [8] [9] is used at the receiver to match the channel and the transmitted waveform. Thus waveform diversity has very broad meaning and significance.

In the context of multi-antenna systems, if there are multiple antennas at the transmitter, this kind of system can explore the spatial diversity and execute transmitter beamforming to focus energy in the desired direction and avoid interference to

other systems. It is well known that waveform and spatially diverse capabilities are made possible today due to the advent of lightweight digital programming waveform generators [10] or arbitrary waveform generators.

Waveform diversity can also be applied to wideband systems. A variety of waveforms with different time-frequency characteristics can be explored in the wideband system to support high data rates, secure property or the resolution and accuracy of radar.

Waveform design for wideband multi-antenna systems are documented in [11]. The equivalent baseband waveforms are designed for passband systems. Different waveforms for different transmitter antennas are jointly optimized to achieve globally optimal performance. At the receiver, the signals from different transmitter antennas will be combined together such that the receive antenna will see only one signal from the transmitter no matter how many transmitter antennas are present. In order to achieve this kind of over the air coherency for the passband signals, all the individual oscillators should be tied together [10] to make the carrier phase consistent.

In the context of cognitive radio, waveform design or optimization gives us more flexibility to design radios, which can coexist with other cognitive radios and primary radios. From a cognitive radio point of view, spectral mask constraints at the transmitter and interference cancellation at the receiver should be seriously considered in waveform design or optimization, in addition to the traditional communication objectives and constraints. Spectral mask constraints imposed on the transmitted waveform such that cognitive radio has no or limited interference to primary radio. At the same time the interference cancellation scheme is implemented at the receiver to cancel the interference from primary radios and cognitive radio.

Even though waveform diversity for radar can be traced back to the World War II, due to the computational capability and hardware limitation, a lot of waveform design algorithms could not be implemented in radar systems [3]. Nowadays, these bottlenecks are broken and waveform diversity becomes a hot spot afresh in the radar society. Time reversal or phase conjugating waveforms, colored waveforms, sparse and regular non-uniform Doppler waveforms, non-circular waveforms and so on are dealt with based on advanced mathematical tools in [12]. New trends in coded waveform design for radar applications are presented in [13]. The modern semidefinite programming (SDP) and novel algorithms on Hermitian matrix rank-one decomposition are exploited to perform code selection which can maximize the detection performance and control the Doppler estimation accuracy and the similarity with a pre-fixed radar code [13]. From here we see that the mathematics is the foundation of the research on waveform diversity. The algorithms from convex optimization and non-convex optimization are exploited most frequently to solve the waveform diversity issue.

Waveform diversity can be applied to wireless tomography. The incident wave or the probing signal can be designed dynamically according to the operating environment and the objective of wireless tomography. Power control–the intelligent selection of transmit power–is one way to deal with waveform diversity in wireless tomography. If background noise of operating environment is big or the working area is large, more power should be allocated to the probing signal to increase signal to noise ratio (SNR) or coverage; otherwise less power should be used in order to lengthen the battery life.

Dynamic spectrum access (DSA) is another way to explore waveform diversity in wireless tomography, especially for the wideband system. Ultra-wideband microwave sensing and imaging is mentioned in [14]. The well known time reversal operator is used. Meanwhile signal space method and null space method are both considered. Multi-frequency inverse scattering is studied in [15]. The object scattering potential is assumed to be independent of frequency over the band of interest [15]. Thus the size of final equations will be determined by the number of transmitter sensors, the number of receiver sensors and the number of frequency points. Wideband microwave tomography with frequency selection is built in [16]. The frequency selection is used to avoid the frequencies where the coupling from the coresident antennas is large enough to prevent successful imaging [16]. No doubt that multi-frequency or wideband wireless tomography can improve the performance of imaging and DSA can give us a way to use frequency band flexibly. If there is a strong interference in certain frequency point, this frequency should be removed for imaging, which is similar to cognitive radio or cognitive radar. The key implementation technology of DSA for wireless tomography is non-contiguous orthogonal frequency division multiplexing (NC-OFDM). NC-OFDM can be used to easily synthesize wideband probing signal with flexible power allocation for sub-carriers.

If more than one transmitter in wireless tomography can emit the probing signals simultaneously, beamforming is the third waveform diversity approach for wireless tomography. As mentioned before, beamforming can focus the incident energy on the targets and increase the strength of scattered field. Besides, for the particular applications, the manifold of transceivers in wireless tomography is arbitrary which poses a challenge for beamforming.

The backbone of wireless tomography is wireless communication and wireless network; while the heart of wireless tomography is the super computing. By super computing, the huge data acquired can be processed quickly and efficiently. Thus sequential waveform design can also be applied to wireless tomography. Several rounds of illuminations will be exploited until quality of tomographic imaging reaches the requirement. The probing signal and the transceiver scheme for each round can be adjustable according to the results of the previous illuminations.

II. Improving Phase Reconstruction Using Machine Learning

Machine learning is a discipline to design algorithms for computers to recognize the complex patterns and make decisions based on training data automatically and intelligently.

However, usually a huge amount of data is fed into the computer which complicates machine learning algorithms. Three major types of machine learning algorithms developed until now are supervised learning, unsupervised learning and reinforcement learning.

The training data of the supervised learning are pairs of input/output(label)

$$(\mathbf{x}_i, y_i), i = 1, 2, \cdots, S \tag{1}$$

where S is the number of training data, in which an intrinsic functional relationship exists mapping inputs to outputs.

Until now, many machine learning algorithms have been proposed such as Nearest Neighbor learning [17], Decision Tree learning [18], Artificial neural networks(ANN) [17] and Support Vector Machine (SVM) [19] [20].

As mentioned before, machine learning usually deals with a large number of data, however, sometimes these data points are highly correlated and redundant with noise. This data model is exactly what we have met in Section I-A.

Methods of dimensionality reduction are innovative and important tools in machine learning [21]. Dimensionality reduction attempts to select or extract a lower dimensionality expression of original data. Principal Component analysis (PCA) [22] is the best-known linear dimensionality reduction method. PCA aims to find a lower dimensionality expression which can maximally maintain the variance of the original data.

PCA works well for the high dimensionality data with linear variability, but always fails when nonlinear nature of data exists. Kernel PCA [23] is, on the other hand, designed to extract the nonlinear structure of the original data. It uses the kernel tricks to map the original data into a feature space $\mathbf{F}$, and then does PCA in $\mathbf{F}$ without knowing the mapping explicitly. We have only applied linear PCA for our problem.

Manifold learning has become a very active topic in nonlinear dimensionality reduction. This approrach will be applied to our problem as well. A lot of promising methods have been proposed, such as Isomeric mapping (Isomap) [24], Local Linear Embedding (LLE) [25], Laplacian eigenmaps [26], Local Tangent Space Alignment (LTSA) [27], Semidefinite Embedding also called Maximum Variance Unfolding (SDE) [28], Hessian eigenmaps [29], Manifold Charting [30], Diffusion maps [31] and Riemannian Manifold Learning (RML) [32]. The basic assumption for these manifold learning algorithms is that the input data lie on or close to a smooth manifold [33] [34].

In wireless tomography, scattered fields are used for imaging. As pointed out above, there are usually a large number of degrees of freedom in the total field [35]. Based on these data, many machine learning algorithms can be applied using the three-step approach suggested above.

A. Principal Component Analysis (PCA)

Our version of PCA algorithm for denoising can be summarized into the following four steps:

Principal Component Analysis (PCA)

1) Given a set of S samples $\mathbf{x}_i \in \mathbf{R}^N, i = 1, 2, \cdots S$, the correlation matrix of this data set is computed by
$$\mathbf{C} = \frac{1}{S} \sum_{i=1}^{S} \mathbf{x}_i \mathbf{x}_i{}^T \tag{2}$$
where T means transpose.
2) Eigenvalues $\lambda_1 \geq \lambda_2 \geq \cdots \geq \lambda_N$ and the corresponding eigenvectors $\mathbf{v}_1, \mathbf{v}_2, \cdots, \mathbf{v}_N$ are derived by decomposing $\mathbf{C}$.
3) The largest eigenvalue and eigenvector are maintained.
4) Denoised $\hat{\mathbf{x}}$ is extracted by $\hat{\mathbf{x}} = \sqrt{\lambda_1}\mathbf{v}_1$.

B. Numerical Results

To save space, we follow the notations in Part I [1] of this series. Imaging targets are enclosed by an investigated circle plane Ω. Both the fields $\mathbf{x}_i$ (inputs) and sites (outputs) y_i information about targets located at different places $i = 1, 2, \cdots, S$ in Ω are collected. Based on the training data, a supervised learning algorithm can be adopted to learn the functional relationship between inputs and outputs and to predict the target's location given any input.

Another example is that dimensionality reduction methods can be used to analyze and denoise the collected data. As a simple example, we apply PCA to denoise phase reconstruction data.

The experiment data is provided by Institute Fresnel in France [36]. The file name is FoamDielIntTM.exp. The working frequency is 2GHz. $a = 0.15$m. $b = 1.67$m. $\theta_i = 0^o$. θ_0 is from 60^o to 300^0 with 1^o interval. The vector $\mathbf{b}$ is used to denote these 241 measurements which are assumed perfectly accurate (true data) with both amplitude and phase information. Here, only amplitudes are measured. In practice, using these low-cost COTS sensors always incorporates measurement errors ("noise") into the true data $|\mathbf{b}|$.

In order to obtain a set of data with higher accuracy, a large number of measurements will be conducted, then these data sets affected by measurement errors are

$$\mathbf{x}_i = |\mathbf{b} + \mathbf{n}_i|, i = 1, 2, \cdots, S \tag{3}$$

where S is the number of measurements.

In the following MATLAB simulation, $S = 2000$. Noise is modeled as

$$\mathbf{x}_i = |\mathbf{b} + \sigma * \mathrm{randn}(241, 1) + j * \sigma * \mathrm{randn}(241, 1)| \tag{4}$$

where $\sigma = 0.05$ and $randn(\cdot)$ is a built-in MATLAB function.

Our three-step approach is demonstrated as follows:

1) Machine Learning Step: The PCA algorithm in Subsection II-A is used to extract a more accurate measurement vector $\hat{\mathbf{x}}$.
2) Phase Reconstruction Step: The algorithm [35] is chosen to execute phase reconstruction task. The algorithm details have been given in Section III of Part I of our series.
3) Coherent Tomographic Processing: Time reversal imaging can be applied in this step.

The reconstruction results are shown in Fig. 1 and Fig. 2 for phase and amplitude, respectively. As seen clearly from these figures, the reconstructed scattered fields using the new three-step approach are much closer to the true scattered fields than using the traditional two-step approach. Indeed, the machine learning step is important to our whole system concept.

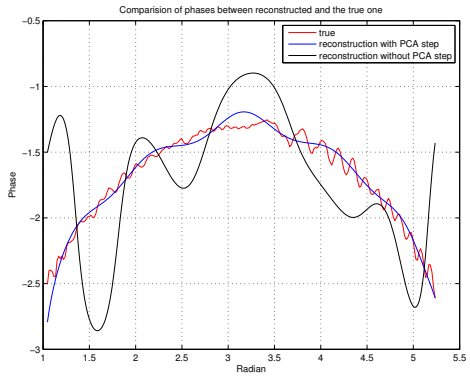

Fig. 1. Phase reconstruction.

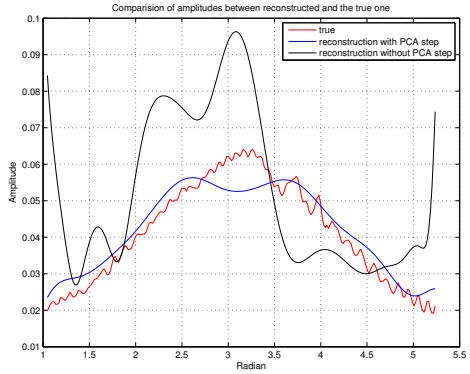

Fig. 2. Amplitude reconstruction.

III. Waveform Diversity in Wireless Tomography

Take the following case as an example to illustrate the benefit of waveform diversity to wireless tomography. The simulation scenario is shown in Fig. 3. There are 30 transceivers represented by the square dots and there is one point target represented by the circle dot. Different from the assumption in [15], the scattering strength of the point target is dependent of frequency. Our goal is to locate the point target in the imaging area and extract the scattering strengths over the frequency band of interest.

Multiple signal classification (MUSIC) algorithm using the background Green's function as steering vector [37] is exploited to yield accurate estimates of the target location. However in order to obtain the scattering strengths over the frequency band, we need to design wideband probing signal to sound the target with the consideration of the background noise in the working area. OFDM waveform will be used as the probing signal and the frequency interval between sub-carriers is determined by the frequency resolution of task

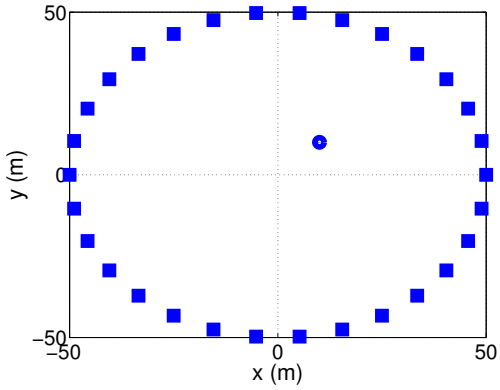

Fig. 3. Simulation scenario for waveform diversity in wireless tomography.

requirement. Thus power allocation to each sub-carrier will be executed in order to get accurate scattering strengths over the frequency band. Assume the frequency points of interest are $f_0, f_1, \ldots, f_N$ and the corresponding wavenumbers are $k_0, k_1, \ldots, k_N$. The scattering strengths related to different frequency points are $\tau_0, \tau_1, \ldots, \tau_N$. There are M transceivers. Thus the measured multistatic data matrix for frequency point f_n is,

$$\mathbf{K}_n = a_n \tau_n \mathbf{g}_n \mathbf{g}_n^T + \mathbf{N}_n \tag{5}$$

where $a_n > 0$ can be treated as the amplitude of the n-th sub-carrier in OFDM waveform. $\mathbf{g}_n$ is the background Green's function vector,

$$\mathbf{g}_n = \begin{bmatrix} G(\mathbf{x}, \beta_1, k_n) \\ G(\mathbf{x}, \beta_2, k_n) \\ \vdots \\ G(\mathbf{x}, \beta_M, k_n) \end{bmatrix} \tag{6}$$

where G is the background Green's function; $\mathbf{x}$ is the estimated location of point target; β_m is the location of the m-th transceiver. $\mathbf{N}_n$ is the background noise matrix for the n-th frequency point. Each entry in $\mathbf{N}_n$ is complex value, the real part and the imaginary part of which both follow Gaussian distribution with zero mean and variance of α_n^2.

Perform vector representation for $\mathbf{K}_n$, $\mathbf{g}_n \mathbf{g}_n^T$ and $\mathbf{N}_n$ to get $\mathbf{k}_n$, $\tilde{\mathbf{g}}_n$ and $\mathbf{n}_n$ respectively,

$$(\mathbf{k}_n)_{l,1} = (\mathbf{K}_n)_{i,j} \tag{7}$$

$$(\tilde{\mathbf{g}}_n)_{l,1} = G(\mathbf{x}, \beta_i, k_n) G(\mathbf{x}, \beta_j, k_n) \tag{8}$$

and

$$(\mathbf{n}_n)_{l,1} = (\mathbf{N}_n)_{i,j} \tag{9}$$

where $(\bullet)_{i,j}$ means the entry of the i-th row and the j-column in the matrix. Thus Eq. (5) turns into,

$$\mathbf{k}_n = a_n \tau_n \tilde{\mathbf{g}}_n + \mathbf{n}_n \tag{10}$$

It is easily from Eq. (10) to see that the noise $\mathbf{n}_n$ degrades the performance. If there is no noise, τ_n can be obtained by $\mathbf{k}_n / (a_n \tilde{\mathbf{g}}_n)$ no matter what a_n is. However if noise exists, we need to choose larger a_n, i.e. more power allocated to the n-th frequency point, to increase the received SNR.

The true scattering strengths are assumed to follow Gaussian distribution with mean of one and variance of $10^{(-4)}$. There are 128 frequency points under investigation. The background noises in the 10-th and the 20-th frequency points are larger than other frequency points around the working area. Set α_{10} and α_{20} to be $10^{(-3)}$. Set other α_n to be $10^{(-9)}$. In the simulation, we assume the total transmitted power $\sum_{n=0}^{N} a_n^2$ is bounded. For power allocation scheme, a_{10} and a_{20} are set to be 100; other a_n are set to be 1. Without power allocation, all a_n are set to be 12.54. Fig. 4 shows the obtained scattering strengths for the first 31 frequency points. From Fig. 4, with simple power allocation scheme that is more power are allocated to the 10-th and 20-th frequency points will give better performance than without power allocation which means power are equally allocated to each frequency point.

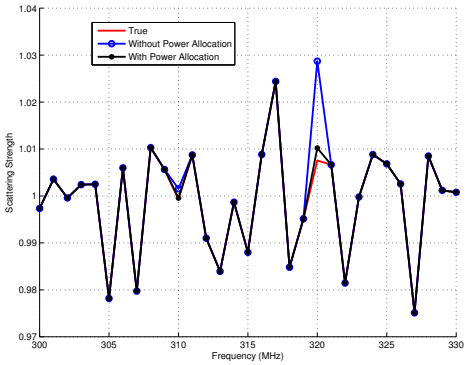

Fig. 4. Obtained scattering strengths over frequency band.

IV. System Testbed Architecture

In order to successfully create an image of what is contained in a room full of RF waves, one might think that extremely complex, sophisticated equipment must be utilized. This, however, may not be the case. A system containing only simple communication equipment very similar to a cellular phone, or even Wi-Fi contained in practically every laptop computer on the market today. Communication signals and radio broadcasts are constant yet invisible forces that are almost always surrounding us in any populated location. There is much more information contained in the interaction of these fields that describes the environment, not only the signal being transmitted.

An experimental set up shown in Fig. 5 to mimic the communication methods of these devices and begin to analyze the properties of these signals as they are attenuated through reflection, refraction, and absorption off of various shaped objects throughout the environment. To mimic the communication nodes of the system, the Universal Software Radio Peripheral 2 (USRP2) has been chosen because of its low cost, open-source software interface, quick learning curve, and daughterboard spectrum flexibility. A single USRP2 can cost anywhere from $\$1,500$ to $\$2,500$, depending on which RF daughterboard is used. The USRP2 can be used to transmit and receive multiple types of communication signals, such as OFDM, DBPSK, DQPSK, and other QAM signals. However, it is limited to relatively narrow band (about 12 MHz), wideband is not permitted currently.

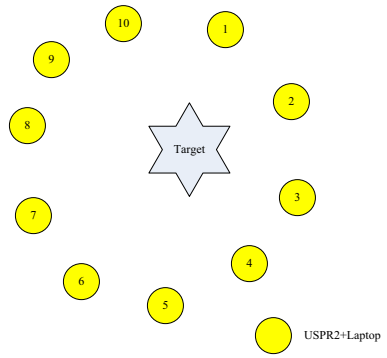

Fig. 5. An experiment set up.

Each USRP2 requires a dedicated host computer, connected via an Ethernet interface. This may not be used for an internet connection while controlling the USRP2. One possible solution is that a laptop be used, which can access the internet through a Wi-Fi, thereby freeing up the use of the Ethernet port. The laptop is set up to boot Linux with a complete GNU Radio installation, including GNU Radio Companion (GRC). GRC is a graphical user interface similar to NI LabView or Mathworks Simulink that contains a variety of signal processing blocks capable of modulating and demodulating the signal sent to a USRP2. GRC also contains graphical sinks that include a signal scope, FFT monitor, as well as a real-time numerical sink. All of these features were utilized in creating the program to control the USRP2.

The USRP2s should be set up to act as a transceiver, each with their own pair of antennas, TX and RX. We used a pair of omnidirectional SMT-8TO25M-A antennas from Skycross. The number of sensing nodes determines the number of USRP2s necessary to conduct the experiment, and each must be paired an individual laptop. From our testing, in order to operate a USRP2 in full duplex mode, a computer with a dual-core processor with a clock speed of at least 2 GHz, as well as at least 2 GB of RAM. If these specifications are not met, than the USRP2 will begin to drop packets, making the measured data useless, as the received waveform will be distorted.

V. Conclusion

When COTS communication components are used, measurement errors in amplitude (attenuation) are difficult to control. As a result, this is a basic problem using our new architecture of using phase reconstruction to retrieve the phase. Since the size of sample space in phase reconstruction is large, machine learning can be applied to reduce the dimensionality

of dimensions—thus reducing the effect of COTS communication components. The random errors introduced by the COTS components tend to be infinite, compared with the finite dimensions. Thus, we introduce a new step called machine learning, before the phase reconstruction step and the coherent tomographic processing step are applied. The new three-step approach works much better than the traditional two-step phase reconstruction approach. Indeed, affordable computing and low-cost COTS communication sensors are behind this three-step approach. We can trade the big number of COTS sensors for the expensive Ad Hoc sensors.

OFDM waveform can be used for the probing signal in time reversal MUSIC. We have demonstrated that waveform diversity improves the reconstructed scattering strength. The same idea is to be applied to phase reconstruction.

System testbed architecture is described. The amplitude of the total field is to be used for phase reconstruction. The experimental results will be reported elsewhere.

Compressive sensing is important to wireless tomography. Short-range ultra-wideband (IEEE 802.15.4a) sensors have capabilities for both communications and localization. When these sensors are considered for wireless tomography, compressive sensing will be very useful. This connection is made in [38], through a multiple input, multiple output (MIMO) context.

REFERENCES

[1] R. Qiu, M. Wicks, Z. Hu, L. Li, and S. Hou, "Wireless Tomography (1): A NovelApproach to Remote Sensing," in *5th International Waveform Diversity & Design Conference*, 2010.

[2] R. Qiu, Z. Hu, M. Wicks, L. Li, S. Hou, and L. Gary, "Wireless Tomography (2): A System Engineering Approach," in *5th International Waveform Diversity & Design Conference*, 2010.

[3] A. D. Maio and A. Farina, "Waveform Diversity: Past, Present, and Future." A Lecture Series on Waveform Diversity for Advanced Radar Systems, July 2009.

[4] N. Guo, J. Q. Zhang, P. Zhang, Z. Hu, Y. Song, and R. C. Qiu, "UWB Real-Time Testbed with Waveform-Based Precoding," in *IEEE Military Conference*, (San Diego, USA), November 2008.

[5] N. Guo, Z. Hu, A. S. Saini, and R. C. Qiu, "Waveform-level Precoding with Simple Energy Detector Receiver for Wideband Communication," in *IEEE Southeastern Symposium on System Theory*, (Tullahoma, USA), March 2009.

[6] Z. Hu, N. Guo, and R. C. Qiu, "Wideband Waveform Optimization for Energy Detector Receiver with Practical Considerations," in *IEEE International Conference on Ultra-Wideband*, (Vancouver, Canada), September 2009.

[7] Z. Hu, N. Guo, and R. C. Qiu, "Wideband Waveform Optimization with Energy Detector Receiver in Cognitive Radio," in *IEEE Military Conference*, (Boston, USA), October 2009.

[8] H. Song, W. Hodgkiss, and S. Kim, "Performance prediction of passive time reversal communications," *The Journal of the Acoustical Society of America*, vol. 122, p. 2517, 2007.

[9] H. Song, W. Hodgkiss, W. Kuperman, W. Higley, K. Raghukumar, T. Akal, and M. Stevenson, "Spatial diversity in passive time reversal communications," *The Journal of the Acoustical Society of America*, vol. 120, p. 2067, 2006.

[10] M. C. Wicks, "History of Waveform Diversity and Future Benefits to Military Systems." A Lecture Series on Waveform Diversity for Advanced Radar Systems, July 2009.

[11] Y. Song, Z. Hu, N. Guo, and R. C. Qiu, "Real-time MISO UWB Radio Testbed and Waveform Design." submitted to IEEE SoutheastCon 2010.

[12] F. Barbaresco, "New Agile Waveforms Based on Mathematics and Resources management of Waveform Diversity." A Lecture Series on Waveform Diversity for Advanced Radar Systems, July 2009.

[13] A. D. Maio and A. Farina, "New Trends in Coded Waveform Design for Radar Applications." A Lecture Series on Waveform Diversity for Advanced Radar Systems, July 2009.

[14] M. Yavuz and F. Teixeira, "Ultrawideband Microwave Sensing and Imaging Using Time-Reversal Techniques: A Review," *Remote Sensing*, vol. 9, pp. 466–495, 2009.

[15] M. Dennison and A. Devaney, "Inverse scattering in inhomogeneous background media: II. Multi-frequency case and SVD formulation," *Inverse Problems*, vol. 20, p. 1307, 2004.

[16] C. Gilmore, S. Noghanian, L. Shafai, S. Pistorius, J. Lovetri, P. Mojabi, A. Zakaria, M. Ostadrahimi, and C. Kaye, "A Wideband Microwave Tomography System with a Novel Frequency Selection Procedure.," *IEEE transactions on bio-medical engineering*, 2009.

[17] T. Mitchell, "Machine learning. 1997," *Burr Ridge, IL: McGraw Hill*.

[18] J. Quinlan, "Induction of decision trees," *Machine learning*, vol. 1, no. 1, pp. 81–106, 1986.

[19] C. Burges, "A tutorial on support vector machines for pattern recognition," *Data mining and knowledge discovery*, vol. 2, no. 2, pp. 121–167, 1998.

[20] A. Smola and B. Schlkopf, "A tutorial on support vector regression," *Statistics and Computing*, vol. 14, no. 3, pp. 199–222, 2004.

[21] J. Lee and M. Verleysen, *Nonlinear dimensionality reduction*. Springer Verlag, 2007.

[22] I. Jolliffe, *Principal component analysis*. Springer verlag, 2002.

[23] S. Mika, B. Scholkopf, A. Smola, K. Muller, M. Scholz, and G. Ratsch, "Kernel PCA and de-noising in feature spaces," *Advances in neural information processing systems*, vol. 11, no. 1, pp. 536–542, 1999.

[24] J. Tenenbaum, V. Silva, and J. Langford, "A global geometric framework for nonlinear dimensionality reduction," *Science*, vol. 290, no. 5500, p. 2319, 2000.

[25] S. Roweis and L. Saul, "Nonlinear dimensionality reduction by locally linear embedding," *Science*, vol. 290, no. 5500, p. 2323, 2000.

[26] M. Belkin and P. Niyogi, "Laplacian eigenmaps for dimensionality reduction and data representation," *Neural computation*, vol. 15, no. 6, pp. 1373–1396, 2003.

[27] Z. Zhang and H. Zha, "Principal manifolds and nonlinear dimension reduction via local tangent space alignment," *SIAM Journal of Scientific Computing*, vol. 26, no. 1, pp. 313–338, 2004.

[28] K. Weinberger and L. Saul, "Unsupervised learning of image manifolds by semidefinite programming," *International Journal of Computer Vision*, vol. 70, no. 1, pp. 77–90, 2006.

[29] D. Donoho and C. Grimes, "Hessian eigenmaps: Locally linear embedding techniques for high-dimensional data," *Proceedings of the National Academy of Sciences*, vol. 100, no. 10, p. 5591, 2003.

[30] M. Brand, "Charting a manifold," *Advances in Neural Information Processing Systems.*, pp. 985–992, 2003.

[31] R. Coifman and S. Lafon, "Diffusion maps," *Applied and Computational Harmonic Analysis*, vol. 21, no. 1, pp. 5–30, 2006.

[32] T. Lin, H. Zha, and S. Lee, "Riemannian manifold learning for nonlinear dimensionality reduction," *Lecture Notes in Computer Science*, vol. 3951, p. 44, 2006.

[33] H. Seung and D. Lee, "The manifold ways of perception," *Science*, vol. 290, no. 5500, pp. 2268–2269, 2000.

[34] H. Murase and S. Nayar, "Visual learning and recognition of 3-D objects from appearance," *International Journal of Computer Vision*, vol. 14, no. 1, pp. 5–24, 1995.

[35] L. Crocco, M. DUrso, and T. Isernia, "Inverse scattering from phaseless measurements of the total field on a closed curve," *Journal of the Optical Society of America A*, vol. 21, no. 4, pp. 622–631, 2004.

[36] J. Geffrin, P. Sabouroux, and C. Eyraud, "Free space experimental scattering database continuation: experimental set-up and measurement precision," *inverse Problems*, vol. 21, p. S117, 2005.

[37] A. Devaney, E. Marengo, and F. Gruber, "Time-reversal-based imaging and inverse scattering of multiply scattering point targets," *The Journal of the Acoustical Society of America*, vol. 118, p. 3129, 2005.

[38] P. Zhang and R. Qiu, "A Compressed Sensing Based Sensing Method for UWB Channel Recovery Considering Pulse Distortion," in *5th International Waveform Diversity & Design Conference*, 2010.